Modeling and Classification of Mountain Waves

A. Tokgozlu
Süleyman Demirel University
Faculty of Sciences and Literature Department of Geography
32260, Isparta, Turkey
tokgozlu@fef.sdu.edu.tr

M. Rasulov
Beykent University, Faculty of Science and Letters
34900, B.Çekmece, Istanbul, Turkey
mresulov@beykent.edu.tr

Z. Aslan
Anadolu BİL Professional School of Higher Education
Computer Technology and Programming
34180,Bahçelievler,İstanbul, Turkey
zaferaslan@anadolubil.edu.tr

XXVII OSTIV Congress, Leszno, Poland, 2003

Abstract

Simulation and analysis of mountain waves in the troposphere are presented in this paper. The shallow water theory was applied to investigation of fluid flows over an isolated ridge. The results of one – dimensional, time - dependent shallow water equations are discussed. These equations have governed the motion of an incompressible, homogeneous, inviscid and hydrostatic fluid. This model gives a crude representation of atmospheric flow. Low level atmospheric gravity waves (inertial waves) are also analyzed by considering radiosonde observations in Isparta (Turkey). The atmospheric component, which reflects the air temperature fluctuations, is referred to as gravity wave variance. Vertical variation of air temperature, relative humidity, and horizontal wind speed components and patterns that are associated with mountain wave observations are discussed.

Introduction

Background

Mountain waves (lee waves) are atmospheric internal gravity waves and were discovered in 1933 by German glider pilots above the Riesengebirge. Wind driven air parcels hitting a mountain-like obstacle are being deflected upwards and will, in a stably stratified atmosphere, return to their initial height setting up an oscillatory up-down motion. Such a wave system which often exhibits typical phenomena as interference and wave breaking is frequently made visible by stationary, lens shaped clouds, called lenticulars, [1].

There are several sources of waves, which can be used by sailplanes. The strongest waves are found above and in the lee of mountains and have been termed "mountain waves "or "lee waves", [2-5]. On shorter time scales, regional mountain chains are an enhanced source of synoptic disturbances, with numerous airborne field projects in instrumentation of motor gliders in atmospheric sciences, [6-9]. The Mountain Wave Project was conceived during an OSTIV seminar in 1998 in Serres, France, by Rene Heise and Klaus Ohlmann. Physicist Wolf D. Herold, who has played a crucial role, both, as scientist and pilot in the Thermal Wave Project carried out at NCAR (National Center for Atmospheric Research, Boulder, Colorado) and meteorologist Carsten Lindemann (Free University of Berlin), a specialist in airborne measurement and remote sensing, who provided sensors and data recording system have significantly contributed to this field.

Lee waves in the Andes Region were analyzed together with knowledge about the meteorological conditions of the South American Andes, [10]. Global classification of mountain waves and their associated rotor bands were analyzed [11]. The main goal of this study is to detect and determine physical processes in the atmosphere and associated synoptic characteristics which play a dominant role in the generation and development of mountain waves.

Atmospheric conditions of stratospheric mountain waves for soaring by The Perlan Sailplane to 30km were studied, [12]. The primary project objective was to attain measurements that lead to better understanding of mountain waves and their effects in altering the stratospheric global circulation. Wind, temperature and updraft measurements will characterize the wave development and propagation; therefore the Perlan Sailplane was used as a measurement source augmented by a temperature and speed sensor.

Another study on non-linear shallow fluid flow over an isolated ridge was carried out, [13]. They use the one-

dimensional, time-dependent "shallow water" equations that govern the motion of an incompressible, homogeneous, inviscid and hydrostatic fluid. This model gives a crude representation of atmospheric flow. The asymptotic mathematical solutions of the model equations are determined for the case where the fluid initially at rest is impulsively accelerated to a velocity which is constant in the space coordinate. The jump on the windward side of the ridge always moves upstream. The jump on the lee side moves down-stream in the domain and remains stationary over the lee slope of the ridge. They investigated the nature of the hydraulic jumps in flows across a ridge.

In fact, Kuettner attempted to use the concept of "jump" in hydraulics to explain the appearance of rotor clouds in the lee of mountains, [14].

The Alpine orography has been simplified to an arch-shaped obstacle of the same size and the wind, blowing from the south, is uniform upstream of the mountain, [15]. Numerical investigation of dry and moist airflow regimes over idealized Alps were presented in this paper.

Observations and analyses of mesoscale gravity waves in the stratosphere from the Upper Atmosphere Research Satellite (UARS) Microwave Limb Sounder (MLS) are summarized by Jiang and his group, [16]. This paper focuses on global distribution of topography-related wave activities. Mountain Waves in the Middle Atmosphere: Microwave Limb Sounder (MLS) observations and analyses are summarized in this study. MLS observations suggest that these orographic waves are located mostly on the down-stream side of the mountain ridge with downward phase progression and have horizontal phase velocities opposite to the stratospheric jet-stream.

There are many situations where dynamic soaring technique can provide an extra source of energy for the glider pilot. The general rule for getting energy from the atmosphere is to push on the air opposite to its direction of motion and remember that faster moving air yields proportionally more energy for the same amount of push, [17]. An increase of wind speed with height without much change of wind direction adds to the likelihood of wave formation, [18].

Objectives

The main goal of this study is to model and analyze mountain waves and their rotor bands, to determine their location, spatial extension and to classify contaminant turbulence. This paper presents a computer simulation of shallow layer dynamics by using finite differences.

Material and Methodology

The best mountain wave conditions required to get to higher altitudes are [2].

- strong low-level winds in a stable atmosphere for initial perturbation by mountains,
- a gradual wind increase with altitude to supply energy for wave amplification,
- a weak tropopause that allows for wave passage,
- High – altitude stratospheric winds (polar vortex) with increasing velocity with altitude.

Study Area

Study area, (Isparta; latitude: 37° 50' N, longitude: 30° 33' E, height, 1200 m. above msl.) is in the south western Anatolia, (Fig. 1). This area is referred to the Area of Lakes. This region is under the effect of central and south western Anatolian climatological conditions. It is under the combined effects of Mediterranean and terrestrial climate conditions with hot and dry summers and cold and wet winters. Annual rainfall is 600mm in Isparta. Complex topography causes orographic and convective rain formation and mountain wave clouds in the observed area, [19].

Data

Daily radiosonde data recorded at Isparta Meteorological station at 00:00GMT in 1995 was analyzed to define mountain wave characteristics over Isparta in 1995. Air temperature, relative humidity and horizontal wind speed values observed at 1000hPa, 850hPa, 700hPa, 500hPa pressure levels were considered for case studies.

Model

Input data of the computer modeling are potential temperature, horizontal wind speed and humidity based on the radiosonde observation for Isparta Region (Davras Mountain, Turkey). The atmosphere is idealized as a two-layer structure, where each of the two atmospheric layers has a uniform profile. Details of the diagnosis of turbulence from an operational numerical model and on the simulation of the event with 2-D numerical model using time – dependent lateral boundary conditions are presented below [20-23].

Horizontal fluid dynamics structure in which a stratified fluid at a speed of u encounters an obstacle and which forces some fluid parcels to move vertically against gravity is studied with the following 2-D model [22, 23]. A simplified atmospheric state, no rotation $f=0$ and $\rho_0 =$ const is assumed. The linearized anelastic equations take the form of nonlinear wave form as below:

$$\frac{\partial u}{\partial t} + u\frac{\partial u}{\partial x} = \frac{\partial P}{\partial x}, \qquad (1)$$

$$\frac{\partial \theta}{\partial t} + u\frac{\partial \theta}{\partial x} + w\Gamma = 0 \qquad (2)$$

where $\theta = \theta(x,z,t)$, $\Gamma = d\theta(z)/dz$, $P = c_p\theta\pi$.

If the initial wind speed or potential temperature profile has negative and positive slope, the solution of Eq. 1 has discontinuous points whose positions are unknown beforehand, [20]. In addition to this, since the equations (1), (2) are nonlinear; there are no classical solutions for them. Furthermore, only a numerical solution can be found. But, due to the properties of function u, the equation (1) can not be approximated by the finite difference scheme. In order to obtain the solution of the equation (1) in a class of

discontinuous functions, the following auxiliary equation is suggested, [21].

$$\frac{\partial v}{\partial t} + \frac{1}{2}u^2 = P, \qquad (3)$$

Where, $v(x,t) = \int u(\xi, z, t)d\xi + C$. In this case the function u can be discontinuous too.

The 2-Dimensional model, which includes the time variable, estimates the drag of the mountain wave that is exerted on the atmosphere. One output of the model is the breaking pressure drag. It varies between 1 and 5 hPa and these values show from light – moderate to severe turbulence intensity respectively.

Analysis

Analysis of Model Outputs

Figures 2-4 show the model results of h (height) values variations for different normalized time stages (for T= 0.8, 1.0 and 1.5). h and T values are normalized values with respect to mean values of height and time intervals. In the initial stage, the normalized h values increase from 1.104 up to 1.221 over the windward side of the simulated mountain. The minimum values over lee side of the mountain show a decreasing trend from 0.86 down to 0.81.

The 2-D model described earlier shows the u-component of the wind (zonal) and time. To compute the zonal and meridianal wind speed components, wind direction was accounted. Variation of normalized horizontal wind speed values (zonal and meridianal components), over the simulated mountain ridge at three stages are presented in Figs. 5 - 7. In the initial stage (for T=0.8), $u_{i,k}$ values vary between 0.9 and 1.05. In the final stage, they vary between 0.8 and 1.15.

Figure 8 shows the simulation of normalized horizontal wind speed values over the mountain.

Simulation of normalized wave amplitudes (h) over a mountain in three different time domains (T = 0.8, 1.0 and 1.5) is presented in Fig. 9. Gradients show the perturbations caused by up winds and down winds over the mountain at the three time stages depicted in Fig. 8.

Analysis of Radiosonde Observations

Figure 10(a) presents the vertical variation of zonal wind speed components over study area in April 1995. Mountain waves were observed on 10th and 15th April. It can be seen from the figure, the mountain waves are accompanied by westerly winds. Wind speed values increase up to 500hPa pressure level. Vertical variation of meridianal wind speed in Isparta, in April, 1995 is shown in Fig. 10 (b). Northerly wind speed components were observed with extreme values at 700hPa and 500hPa pressure levels corresponding to the observed mountain wave events. Vertical variation of relative humidity values is presented in Fig. 10 (c) in the same period over Isparta. Increasing values of relative humidity observations are accompanied with low and medium level wave clouds. Upper layer temperature values increase at 850hPa pressure level, (Fig. 10 (d)). They indicate stable stratification below 700hPa pressure level and low level inertial gravity waves, i.e. mountain waves over the study area on 10th and 20th of April, 1995. The results of actual data analysis show similarities with other mountain wave observations in 1995 over Isparta.

Results and Conclusions

The model produces spatial variation and a contour plot of horizontal wind speed. The vertical propagation of the waves is shown (Figs. 2 to 4). The normalized horizontal wind speed component variations based on theoretical model analysis successfully shows the trapped waves producing alternating regions of subsidence and ascent (Fig. 9). The results of this paper have been compared to the results of a previous study on graphical method, [3]. Dynamical model results on wave characteristics reported here show a better approximation to the real atmospheric conditions than the graphical methods. Comparison of increasing amplitude values based on model simulations to normalized horizontal wind speed component shows similar structure around 700hPa pressure level. Interpretation of meteorological data and model simulations and the results of this study will provide the crucial input for the meteorological aspects of glider flights planning.

Acknowledgements

The authors would like to express their gratitude to Lecturer H. Övgü TÜZÜN and Mr. Onur TAŞCAN for their contributions.

References

[1] Pagen, D., *"Understanding The Sky: A Sport Pilot's Guide to Flying Conditions,"* p.p. 280, ISBN 0-936310-03, USA, 1992.

[2] WMO, Handbook of Metrological Forecasting For Soaring Flight. WMO, Technical Note 158, 1993.

[3] Aslan, Z. and Tokgözlü, A., "Mountain Waves and Gliding," *UCANTURK*, June, pp. 6-10, Ankara, 1990, (in Turkish).

[4] Aslan, Z. and Tokgözlü, A., "Instability Indices for Atmospheric Convection," XXVth. OSTIV Congress, July 7-11, St. Auban, France, 1997.

[5] Oğuz, O., Aslan, Z., and Yazıcı, D., "Gravity Wave Induced Ionization Layers in the F Region Over Istanbul," EGS XXIV General Assembly, ST, 195, pp. 19-23, The Hague, April 1999.

[6] Lindeman, C., "Soaring Climatology of Thermal Convection," *Technical Soaring*, Vol. 12, No. 3, pp. 95-100, 1993.

[7] Reinhardt, M.E., Neininger, B., Kuettner, J.P., Adhikary, S.P., and Lert, P.S., "First Results of Airborne Measurements of the Mountain Valley Circulation in the Kali Gandaki

Valley, Nepal, by Motorglider," *OSTIV Publication XVII*, pp. 158-163, 1985.

[8] Heise, R., "Mountain Wave Project," 1-28 OSTIV Scientific Section and Meteorological Panel, DLR, November 2001.

[9] Heise, R., "MWP: Mountain Wave Project," p. 7, 2004. http://www.mountain_wave_project.de, Germany.

[10] Lindemann, C., Heise, R., and Herold, W.D., "Lee Waves in the Andes Region, Mountain Wave Project (MWP) of OSTIV," XXVI OSTIV Congress, Mafikeng, 2001.

[11] Andes, S. M. L., "Mountain Wave Project," Coordinated by Rene Heise, 2003.
http://www.pa.op.dlr.de/ostiv/projects/mwavproj.htm

[12] Teets, E. and Carter, E.J., "Atmospheric Conditions of Stratospheric Mountain Waves: Soaring the Perlan Aircraft to 30km," NASA Dryden Flight Research Center, California, 2003.

[13] Houghton, D., D. and Kasahara, A., "Nonlinear Shallow Fluid Flow Over an Isolated Ridge", *Communications on Pure and Applied Mathematics*, Vol. XXI, pp. 1-23, 1968.

[14] Kuettner, J., "The Rotor Flow in the Lee of Mountains," GRD Research Notes, No. 6, Geophysics Research Directorate, Air Force Cambridge Research Center, (ASTIA Document No. AD 208862), 1959.

[15] Stein, J., "Numerical Exploration of Dry and Moist Airflow Regimes over Idealized Alps," 2003. www.map.ethz.ch/NL15/stain.pdf.

[16] Jiang, H. J., Wu, D.L., Eckermann, S.D., and Ma, J., "Mountain Waves in the Middle Atmosphere: Microwave Limb Sounder Observations and Analyses," Advances in Space Research, C2.1-0008, COSPAR, 2002.

[17] Kiceniuk, T., "Dynamic Soaring and Sailplane Energetics ," *Technical Soaring*, Vol. 15, No. 4, pp. 221-227, 2001.

[18] Wallington, C. E., *Meteorology for Glider Pilots*, The Bath Press, p. 331, 1986.

[19] Tokgozlu, A. and Aslan, Z., "The Study of Wind Energy Potential on The Lake Eğirdir and Possibilities of Utilization," Turkey National Wind Energy Symposium, Vol. 86, pp. 105-108, Istanbul, 1995, (in Turkish).

[20] Whitham, G. B., *Linear and Nonlinear Waves*, Wiley Int., New York, 1974.

[21] Rasulov, M. A., *Finite Difference Scheme for Solving of Some Nonlinear Problems of Discontinuous Functions*, Baku, 1996.

[22] Aslan,, Z., Rasulov, M., and Tokgözlü, A., "Mountain Waves and Soaring," ABMYO Bulletin No. 1, 2006, (submitted, in Turkish).

[23] Rasulov, M., Aslan, Z., and Pakdil, O., "Finite Differences Methods for Shallow Water Equations in a Class of Discontinous Functions," Applied Mathematics and Computation, pp. 343-353, 2005.

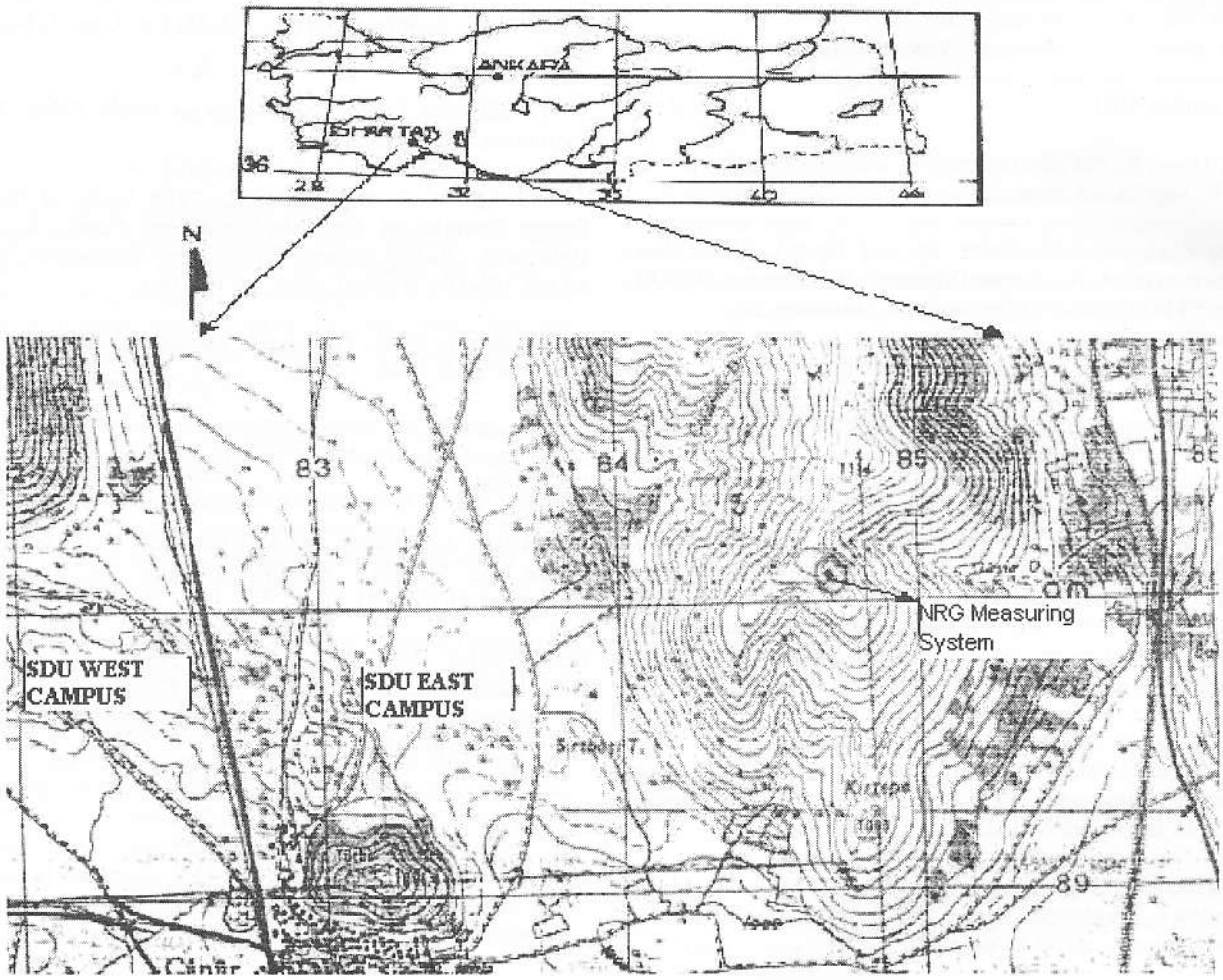

Figure 1 The study area, topographic map and details of the Süleyman Demirel University

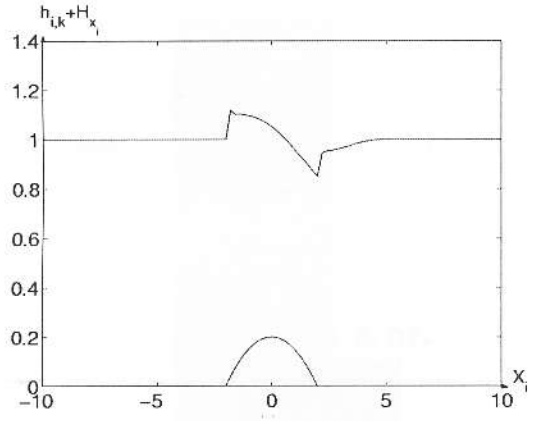

Figure 2 Model results, variation of h values for T = 0.8

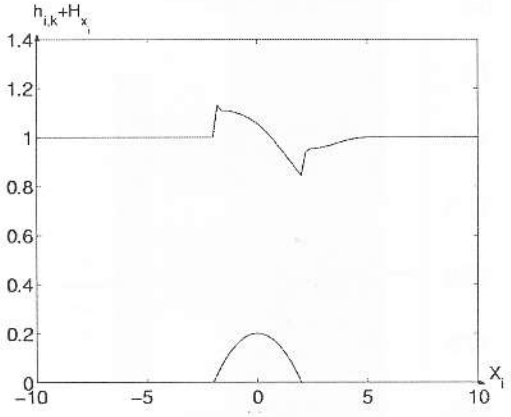

Figure 3 Model results, variation of h values for T = 1.0

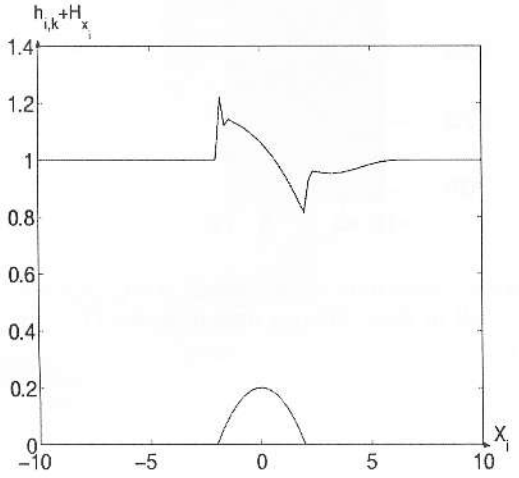

Figure 4 Model results, variation of h values for T = 1.5

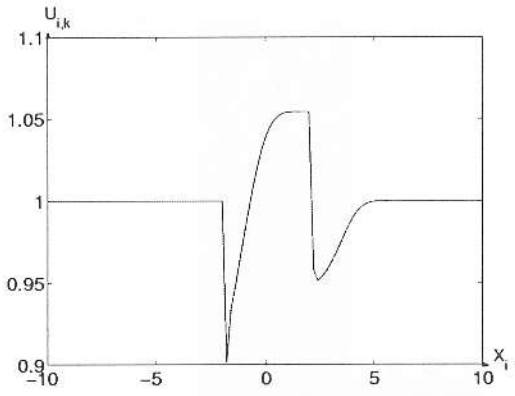

Figure 5 Model results, variation of u values for T = 0.8

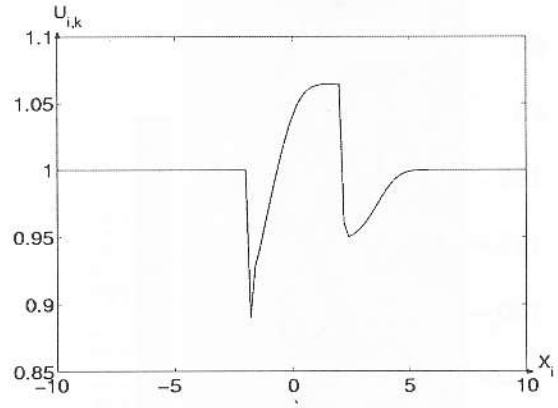

Figure 6 Model results, variation of u values for T = 1.0

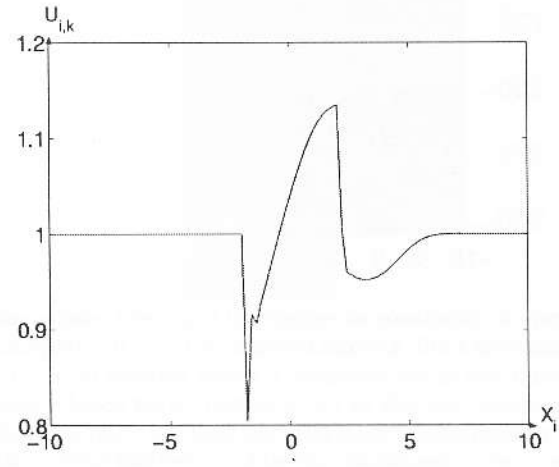

Figure 7 Model results, variation of u values for T = 1.5

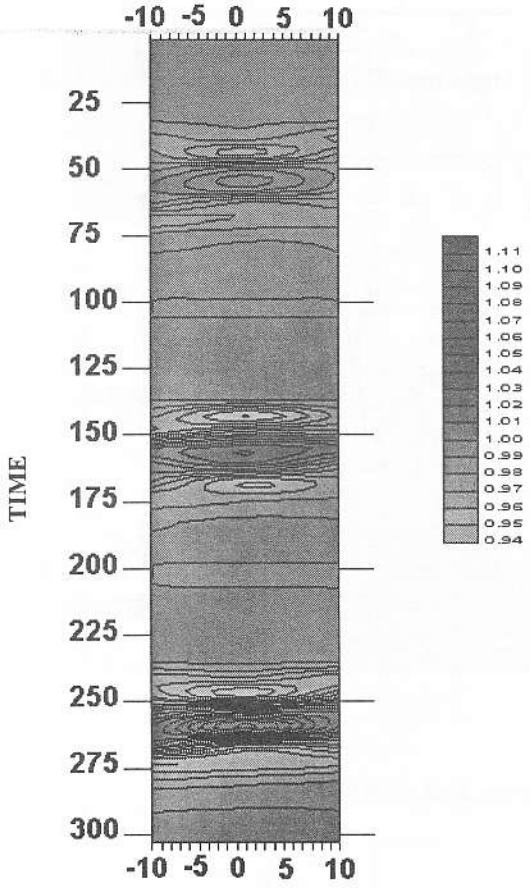

Figure 8 Simulation of normalized horizontal wind speed values over a hill. x values between $-10 < x < 0$ correspond upwind side of the mountain. x values between $0 < x < 10$ correspond lee side of the mountain. Wind speed values are normalized for three different time intervals: i) Upper part of simulation (T=0.8 50<TIME<75), ii) middle,(T=1.0 etc), iii) lower, (T=1.5 etc).

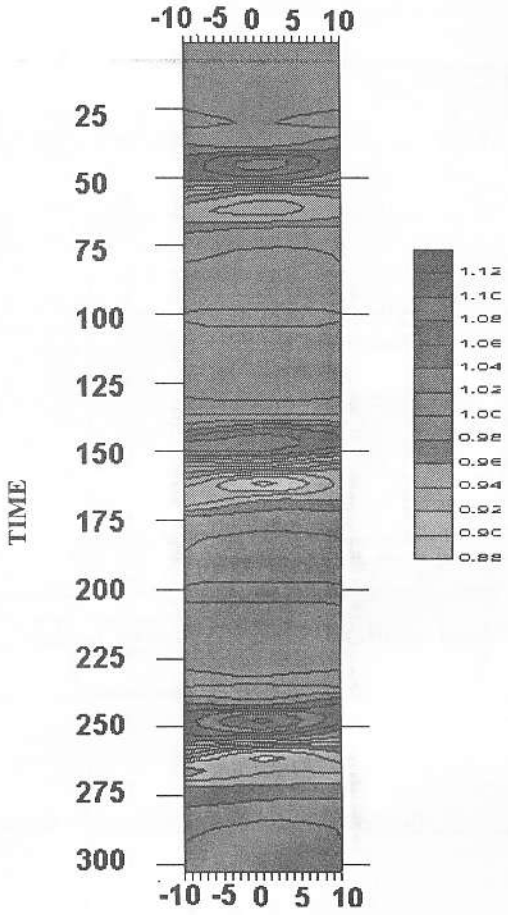

Figure 9 Simulation of normalized wave amplitude (h) over a hill in three different time intervals: (T = 0.8, 1.0 and 1.5).

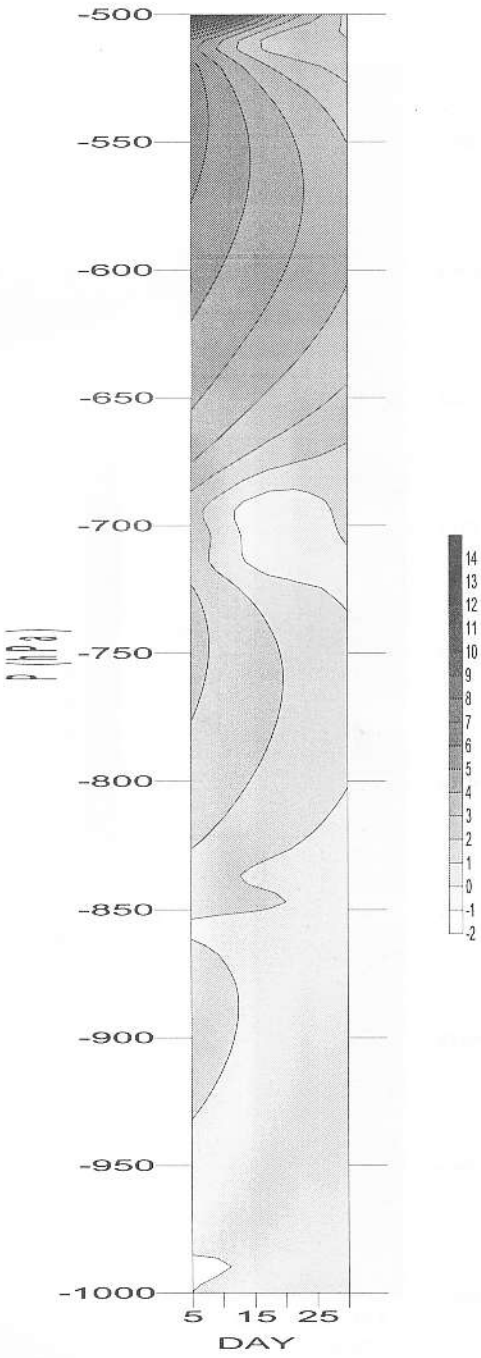

Figure 10 (a) Vertical variation of zonal wind speed (m/s) in April, 1995, in Isparta, (Mountain waves were observed in 10th and 15th April).

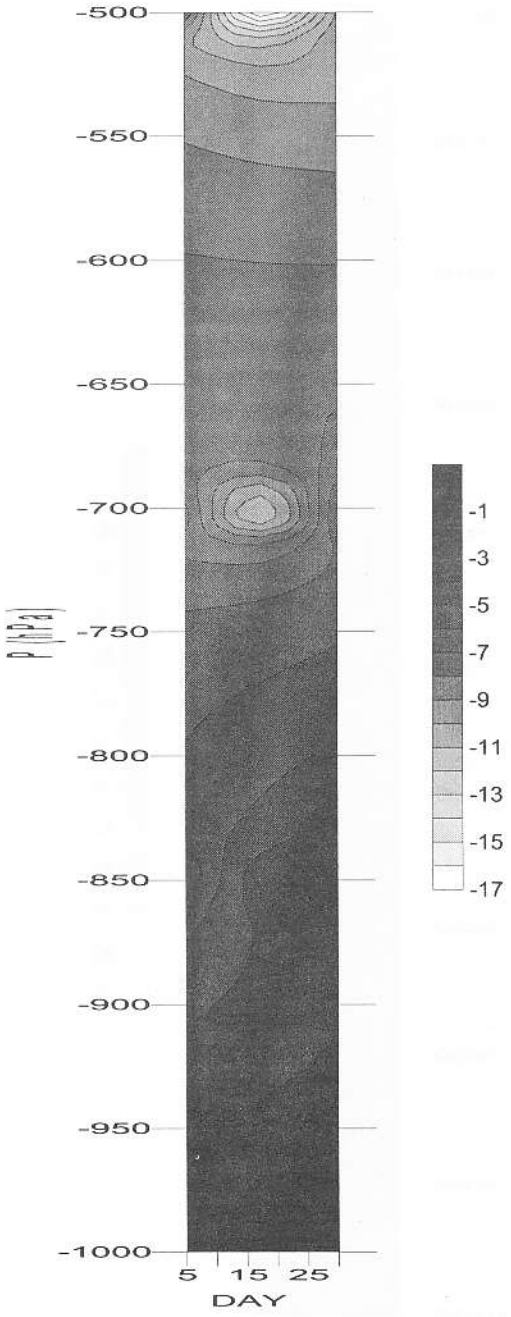

Figure 10 (b) Vertical variation of meridianal wind speed (m/s) in April, 1995, in Isparta.

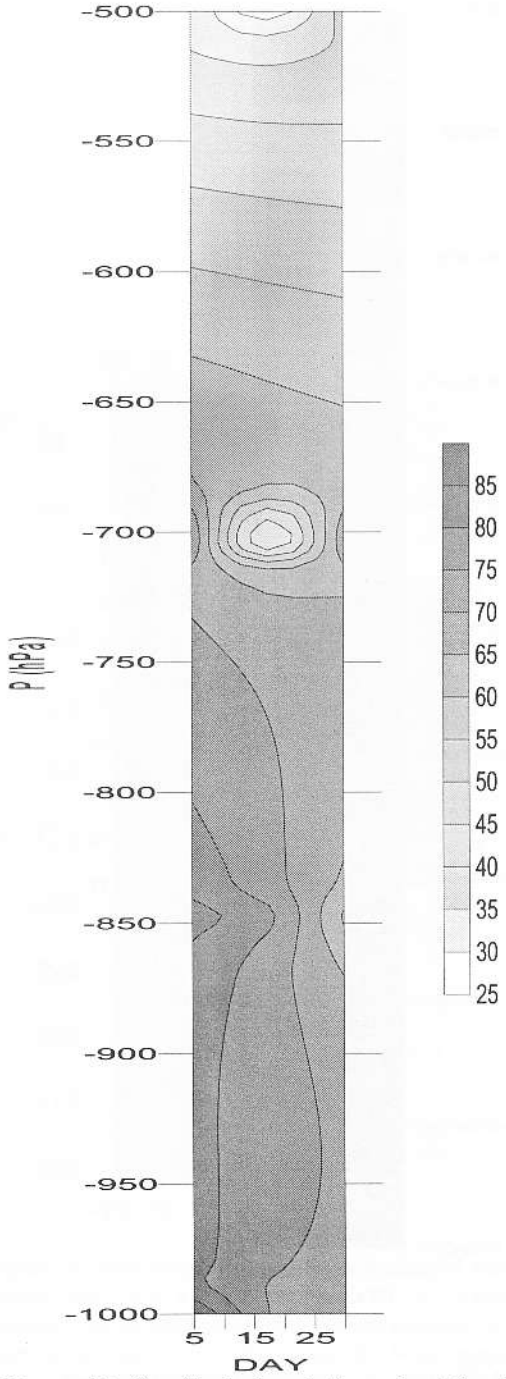

Figure 10 (c) Vertical variation of relative humidity (percent) in April, 1995, in Isparta, (Mountain waves were observed in 10th and 15th April).

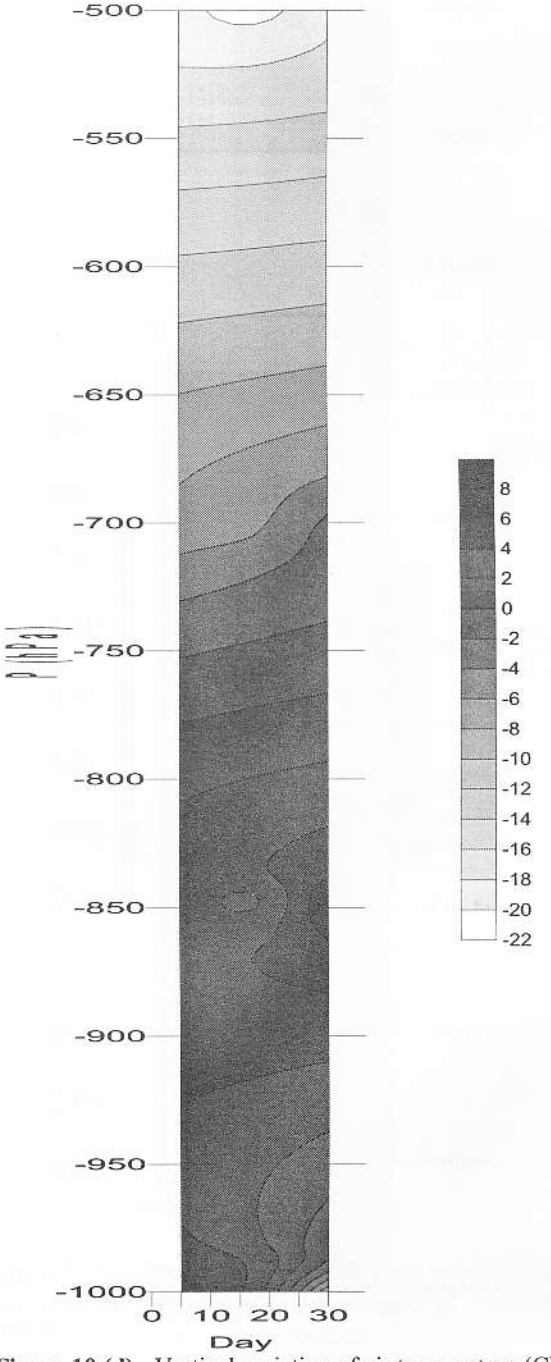

Figure 10 (d) Vertical variation of air temperature (C) in April, 1995, in Isparta, (Mountain waves were observed in 10th and 15th April).